Desalination and Water Treatment
www.deswater.com
doi: 10.1080/19443994.2014.883058

52 (2014) 5084–5091
July

Taylor & Francis
Taylor & Francis Group

Study on the effect of modified PVDF ultrafiltration membrane for secondary effluent of urban sewage

Huang Danxi[a,*], Wang Lei[a], Meng Xiaorong[b], Wang Xudong[b], Bai Juanli[a]

[a]*School of Environmental and Municipal Engineering, Xi'an University of Architecture and Technology, Xi'an 710055, China*
Email: huangdanxi@126.com
[b]*School of Science, Xi'an University of Architecture and Technology, Xi'an 710055, China*

Received 5 December 2012; Accepted 8 March 2013

ABSTRACT

The cross-linked poly(vinyl alcohol) (PVA)/poly(vinylidene fluoride) composite flat sheet membranes were successfully prepared by phase inversion method. Ferric trichloride ($FeCl_3$) particles were used as cross-linker. PVA is cross-linked during the membrane fabrication. The structures of formed membranes were investigated using scanning electron microscopy and Fourier transform infrared spectroscopy (FTIR). The hydrophilic contact angle, pure water flux, and tensile strength were measured to assess the membrane performance. The antifouling performance of modified membrane for the secondary effluent of urban sewage was evaluated by flux decline, washing recovery rate, fouling resistance analysis, and fractions distribution of different hydrophilicities. FTIR showed that the peak intensity, attributed to –OH groups, decrease gradually with the increase of $FeCl_3$, indicating the formation of a PVA–Fe^{3+} net work structure. The addition of cross-linking agent $FeCl_3$ confined the compaction of membranes, thus the fouling resistances of membranes were lower and the water flux was higher. When the weight ratio of PVA to $FeCl_3$ was 1/0.09, the modified membranes had the best UF performance and antifouling property.

Keywords: Antifouling; Cross-linking; Ultrafiltration; Hydrophilic modification; Secondary effluent

1. Introduction

Reclamation of urban sewage has widely been recognized as a reliable and environmentally sensitive means to maximize water resources and reduce the waste of fresh water, the increasing demand of which has resulted in the emergence of water reuse technologies. Recently, ultrafiltration has been used extensively in drinking water and wastewater treatment field [1]. Poly(vinylidene fluoride) (PVDF) is one of the most extensively applied membrane materials for outstanding antioxidation, thermal and hydrolytic stability, as well as good mechanical and film-forming properties [2]. However, hydrophobicity of PVDF has been a barrier for its application in wastewater treatment [3]. In wastewater treatment, a hydrophilic membrane has some obvious advantages. Firstly, an hydrophilic membrane is easily wetted and this results in easy

*Corresponding author.

Presented at the Conference on Water Resources and Urbanization Development, 26–27 September 2012, Tianjin, China

commissioning procedures and high permeabilities relative to the pore size. Secondly, the fouling constituents often present in wastewater sources are organics, which readily attach to a hydrophobic surface. Thus, several approaches have been attempted to improve the hydrophilicity of PVDF membranes, including surface coating [4,5], surface modification [6,7], and blending with hydrophilic polymers [8–10].

It is well known that poly(vinyl alcohol) (PVA) is one of the main hydrophilic polymer additive used for blending with PVDF [11]. It has a high density of –OH function, good membrane forming properties, and good chemical and thermal stability. Besides, PVA can provide a smooth surface. However, the precipitated PVA membrane is still soluble in water during water treatment. Thus, the immobilization of the PVA is essential. To make them into membranes which are insoluble in liquid water and with good tractility, some degree of cross-linking is required during membrane preparation. It is known that under acidic conditions, the hydroxyl groups of PVA react with aldehydes to form acetal or hemiacetal linkages [12]. Li. et al. [9] mentioned that the decrease of mass loss rate and the hydrophilicity of PVDF/PVA membrane resulted from heat cross-link. Du et al. [5] applied a layer of low resistant PVA to a PVDF UF membrane, followed by a solid–vapor interfacial cross-link and an evaluation of its effect on fouling. Godovsky et al. [13] synthesized the nanosized magnetite particles *in situ* within the PVA solution by precipitating Fe^{2+} ions or mixture of Fe^{2+} and Fe^{3+} ions with NaOH solution. Such nanoscale particles homogeneously dispersed in PVA matrix from the three-dimension network structure due to the chelating ability of PVA.

In the previous work, the PVDF/PVA blend membranes were prepared successfully. This research used an easier and cheaper way of cross-linking. Ferric trichloride ($FeCl_3$) particles were used as a cross-linker. PVA was cross-linked during the membrane fabrication. The object of this work is to cast the cross-linked PVA/PVDF composite flat sheet membrane and systematically evaluate the hydrophilic properties, ultrafiltration performance, and its anti-fouling effect on secondary treated water from urban sewage.

2. Experimental methods

2.1. Materials

To prepare the casting polymer solutions, the polymer (PVDF; M_w 573,000, solef1015, Solvay) was used. *N*,*N*-dimethylactamide (DMAc; >99% purity, FuCheng, Tianjing, China) was used as solvent. PVA was purchased from Shanxi Sanwei Co. Ltd, China. $FeCl_3$, polyethylene glycol (PEG, M_w 400), and lithium chloride (LiCl) were obtained from Tianjing FuCheng Reagent Company. Bovine serum albumin (BSA; MW 67,000 Da) was purchased from Lanji, Shanghai, China.

Secondary effluent from the fourth sewage treatment plant (Xi'an, China) was used in the fouling test. The samples were filtrated with 0.45 μm microfiltration to remove particles and insoluble matter. The samples were stored at 5℃ until the experiments were conducted. Before each experiment, the temperature of the samples was adjusted to room temperature.

2.2. Preparation of the modified membrane

The flat sheet membranes have been prepared by phase inversion method. In this study, as shown in Table 1, two kinds of membranes were laboratory prepared: (1) with cross-linking agent $FeCl_3$; (2) without cross-linking agent $FeCl_3$.

Casting dopes were prepared by dissolving the PVDF in the solvent and adding PVA particles, cross-linking agent $FeCl_3$, and other additives to casting solution under stirring. The mixture was stirred at 70℃ for about 24 h to ensure the complete dissolution of the polymer. The resulting homogeneous solution was deposited for one day for removing air bubbles. Each polymer solution was cast over a glass plate at room temperature employing the same casting knife. The cast films were exposed to solvent evaporation for 5 s. Then, the cast films together with the glass plates were immersed in different coagulation bath at 40℃ as presented in Table 1. The formed membranes were washed with and immersed in distilled water until they were used as characterization samples.

2.3. Membrane characterization

The formed membranes were characterized by the methods shown below:

(1) Contact angle between water and the membrane surface was measured using VCA optima (AST products, Inc., MA, USA) as follow: a water droplet is placed onto a flat homogeneous membrane surface and the contact angle of the droplet with the surface was measured. The value was observed until there was no change in contact angle during the short measurement time [14]. At least five measurements of drops at different locations

Table 1
Experimental design for preparation of flat-sheet membranes by phase inversion method

Membrane	PVDF (wt.%)	PVA (wt.%)	PVA/$FeCl_3$ (wt.%/wt.%)	PEG400 (wt.%)	LiCl (wt.%)	DMAc (wt.%)	Coagulation bath
P1	14.4	3.6	1/0	3	3	76	Water
P2	14.4	3.6	1/0.03	3	3	75.9	0.01 mol/L HCl
P3	14.4	3.6	1/0.09	3	3	75.7	0.01 mol/L HCl
P4	14.4	3.6	1/0.15	3	3	75.5	0.01 mol/L HCl

were averaged to obtain CA for one membrane sample.

(2) The cross-section and top surface structures of membranes were observed by using a scanning electron microscope (SEM, JSM5800, Japan, JEOL). The membranes were broken in liquid nitrogen and dehydrated through 50, 75, and 100% (v/v) ethanol, respectively. All dried samples were coated with a thin layer of gold at standard high-vacuum conditions before being tested.

(3) The average pore size of the prepared membranes were determined by the filtration velocity method according to the Guerout–Elford–Ferry equation [15]:

$$r_m = \sqrt{\frac{(2.9 - 1.75\varepsilon) \times 8\eta l Q}{\varepsilon A \Delta P}} \quad (1)$$

where r_m is the average pore size of the prepared membranes (μm), η is the viscosity of permeate flux (Pa s), l is the membranes thickness (m), Q is the pure water flux (m^3/s), A is the effective membrane area (cm^2), ε is the membrane porosity, and ΔP is the transmembrane pressure (0.1 Mpa).

(4) Mechanical properties of hollow fiber membranes were measured by a test machine at a loading velocity of 500 mm/min. The report values were measured three times for each sample and then averaged.

2.4. Water quality analysis

The raw water samples were characterized in terms of UV_{254}, chemical oxygen demand (COD), total organic contents (TOC), pH, turbidity, and molecular weight distribution of organic matter in raw water (Table 4). For analysis method for these parameters, it was reported previously [16].

The hydrophilicity fractions distribution was also tested. First, HCl (1 mol/L) was used to adjust the pH of the samples to 2. Then, raw water was forced through the DAX-8 and XAD-4 resin (America Rohmhass company) adsorption column in turn. Strong hydrophobic fraction was absorbed by DAX-8 resin and weak hydrophobic fraction was absorbed by XAD-4. NaOH (0.1 mol/L) was used to desorb organic matter from the two resins. Hydrophilic fraction passed through the two resins without any adsorption. Then adjust its pH to 8.0 and force it through the IRA-958 resin (America Rohmhass company) adsorption column. The charged hydrophilic fraction was absorbed by IRA-958 resin. Miscible liquids of NaOH (1 mol/L) and NaCl (1 mol/L) were used as eluant. The residual composition was neutral hydrophilic fraction.

2.5. Permeation measurements and antifouling evaluation

All experiments were carried out using a dead-end stirred cell filtration system. The membranes were characterized by pure water flux at 0.1 Mpa transmembrane pressure. The flux was calculated by the following equation:

$$J_w = \frac{Q}{A \times \Delta T} \quad (2)$$

where J_w is pure water flux ($L\,m^{-2}\,h^{-1}$), Q is the volume of water permeated (L), A is effective membrane area (m^2), and ΔT is sampling time (h).

In order to observe membranes fouling condition, membranes were tested in a dead-end ultrafiltration cup fed with secondary effluent of urban sewage from the fourth sewage treatment plant in Xi'an. The flux was decreasing with filtration time increasing due to membrane fouling. Then, the membranes were cleaned with pure water or alkaline solutions after

filtration. The flux recovery ratio (FR) was calculated as the following equation:

$$\mathrm{FR}(\%) = \frac{J_{ww}}{J_{wi}} \times 100 \quad (3)$$

where J_{ww} and J_{wi} are the pure water flux of fouled and fresh membranes, respectively.

The resistance is due to the formation of a cake or gel layer on the membrane surface. The flux (J), through the cake and the membrane, may be described by Darcy's law:

$$J = \frac{\Delta P}{\mu \times R_t} \quad (4)$$

where ΔP is the transmembrane pressure (driving force), μ is viscosity of permeate, and R_t is the sum of the resistances.

The intrinsic membrane resistance (R_m) can be estimated from the initial pure water flux:

$$R_m = \frac{\Delta P}{\mu \times J_{wi}} \quad (5)$$

Fouling resistance (R_f) caused by pore plugging and irreversible adsorption of foulants on membrane pore wall or surface is calculated as:

$$R_j = \frac{\Delta P}{\mu \times J_{ww}} - R_m \quad (6)$$

Cake resistance (R_c) formed on the membrane surface by cake layer [17] can be calculated from the water flux after physical cleaning, which includes water washing and back wash:

$$R_c = \frac{\Delta P}{\mu \times J_m} - R_m - R_f \quad (7)$$

Concentration polarization resistance (R_p) formed on the membrane surface by feed concentration can be calculated from the water flux (J_n) after feed filtration:

$$R_p = R_t - \frac{\Delta P}{\mu \times J_n}$$

where the total filtration resistance (R_t) is the sum of R_m, R_P, R_f, and R_c.

3. Results and discussion

3.1. FIIR studies

Fig. 1(a) shows the Fourier transform infrared spectroscopy (FTIR) spectra of the modified membranes with different weight ratio of PVA to $FeCl_3$. The absorption at around 3,300 cm^{-1} was attributed to –OH vibrations. With the increase of $FeCl_3$, the peak intensity at 3,300 cm^{-1} decreased gradually. This indicated that the cross-linking reaction of PVA and Fe^{3+} occurred. In addition, Fig. 1(b) shows that the adsorption bands at 1,431 and 1,406 cm^{-1} were attributed to the vibrations of C–OH and CF_2. For convenient comparison, the ratio of the intensity of the absorption bands 1,431 cm^{-1} to that of the absorption bands 1,406 cm^{-1}, namely C–OH/CF_2, is used to estimate the change of hydroxyl groups. The results are summarized in Table 2. It was obvious that the C–OH/CF_2 decreased, with the increase of the $FeCl_3$ concentration. The PVA–Fe^{3+} net work structure was formed. The schematic diagram of the interaction between PVA molecules and Fe^{3+} ions was shown in Fig. 2.

3.2. Morphologies of membranes

Fig. 3 shows the top surface and cross-sectional images of the flat-sheet membranes (P1–P4). As can be seen in Fig. 3, the low amount of $FeCl_3$ (P2) resulted in the increase of surface pores compared with PVDF/PVA membrane (P1) and the finger-like voids of P2 membrane are larger than those of P1 membrane. This phenomenon may be interpreted as follows: the degree of cross-linking between PVA molecules and Fe^{3+} was low, the precipitation rate increased with the addition of $FeCl_3$, which favored the formation of a porous structure. However, higher $FeCl_3$ concentration (P3, P4) increased the degree of cross-linking and the dope viscosity, which thereby slowed down the precipitation rate, made the surface denser and caused the finger-like voids smaller than those of P2 membrane.

3.3. Hydrophilicity, pore size, mechanical properties, and pure water flux of membranes

The surface hydrophility was evaluated by water contact, and a higher hydrophilicity give a small contact angle [18]. The contact angle data of modified membranes are shown in Table 3. As revealed by FTIR spectra, the decrease of –OH groups was responsible for the hydrophilicity decrease, which was caused by the cross-linking reaction between the PVA molecules

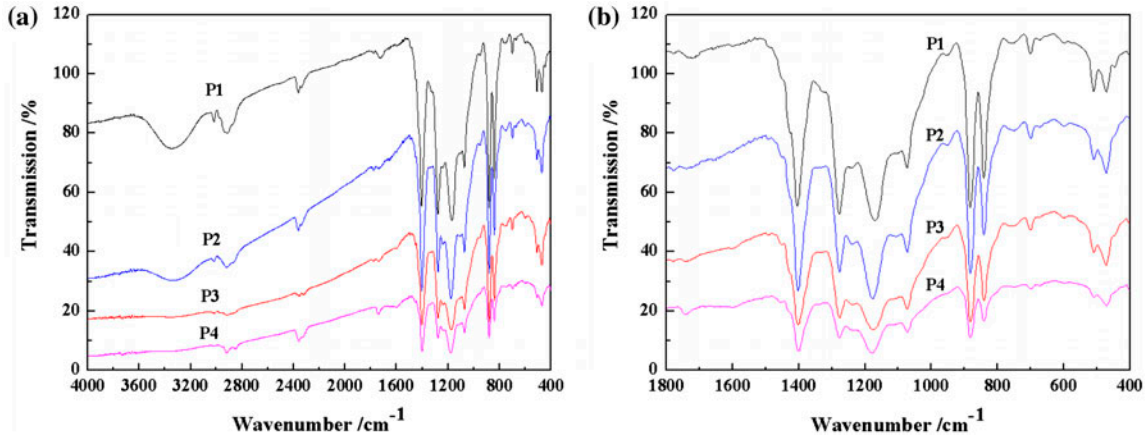

Fig. 1. FTIR spectra of the modified flat sheet membranes.

Table 2
Comparison of the absorption peak intensity of C–OH and CF_2

Membrane	Peak intensity		
	C–OH	CF_2	C–OH/CF_2
P1	33.990	13.661	2.488
P2	50.204	21.697	2.314
P3	60.266	45.574	1.322
P4	73.199	60.959	1.201

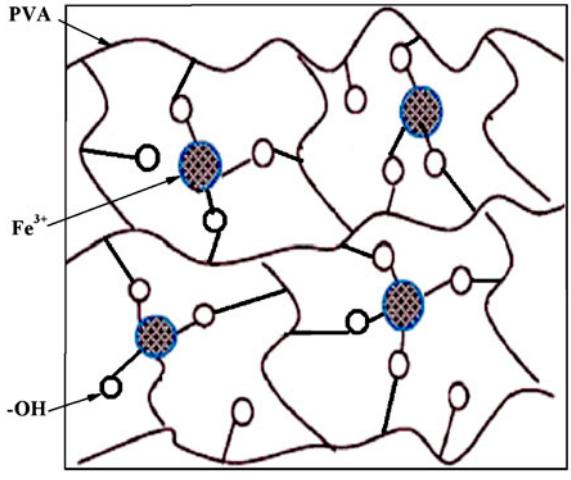

Fig. 2. The schematic diagram of interaction among PVA molecules and Fe^{3+}.

and Fe^{3+}. However, the pure water flux of membranes (P2–P4) was higher than that of P1 membrane. This phenomenon may be interpreted as follows: the addition of crosslinking agent $FeCl_3$ produces a PVA–Fe^{3+} net work structure, which confined the compaction of membranes and consequently suppressed the decline of the pure water during permeation process, higher stable pure water flux of membrane was obtained. The average pore size and tensile strength data of the prepared membranes were also listed in Table 3. The results were consistent with the observation of membrane structure.

3.5. Water quality analysis

The UV_{254}, COD, TOC, pH, turbidity, and molecular weight distribution of organic matter in water samples are listed in Table 4. As can be seen, in the secondary effluent of urban sewage, the organisms with molecular weight less than 10 KDa take the most proportion (64.1%) and the organisms with molecular weight between 30 and 50 KDa are in the next place (19.9%). The rest of the organic molecular weight distribution for each interval is about 5%.

Different hydrophilicity fraction distributions of the secondary effluent are shown in Table 5. As is shown in the table, the strong hydrophobic component accounts for the largest proportion, and then was the charged hydrophilic composition. In addition, the proportions of weak hydrophobic and neutral hydrophilic component are the smallest, which is 9.6 and 10.4%, respectively.

3.6. Fouling test

The secondary effluent from the fourth sewage treatment plant in Xi'an was used to evaluate the fouling behavior of the modified membranes. Fig. 4 shows that the permeation flux of membranes declined with

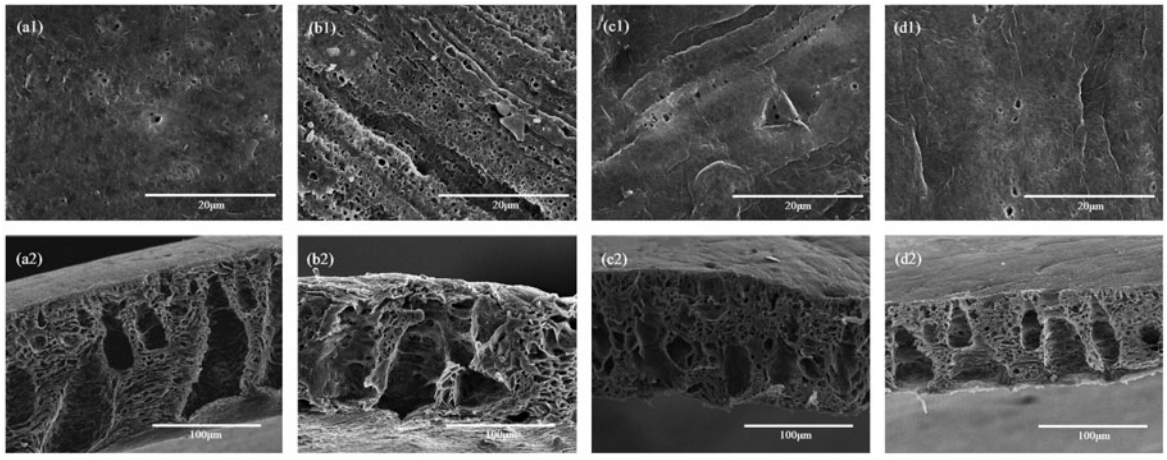

Fig. 3. Top surface and cross-sectional images of the modified flat-sheet membranes ((a) P1, (b) P2, (c) P3, (d) P4; a1–d1: top surface, 3,000×, a2–d2: cross-section, 500×).

Table 3
Contact angle, average pore size, tensile strength, and pure water flux of the modified membranes

Membrane	Contact angle, $\theta/^\circ$	Average pore size, r_m/nm	Tensile strength/MPa	Pure water flux/L/m^2 h
P1	68.5	35.9	2.54	277
P2	66.3	80.1	1.11	1,400
P3	70.2	33.3	1.70	630
P4	75.6	31.1	1.54	500

Table 4
Characteristics of the secondary effluent from the fourth sewage treatment plant (Xi'an)

Parameter	Samples
UV_{254}, cm^{-1}	0.14–0.16
COD, mgL^{-1}	24.6–44.9
TOC, mgL^{-1}	8–10
pH	7–8
Turbidity, NTU	4–10
Molecular weight distribution/%	
<10 kDa	64.1
10–30 kDa	5
30–50 kDa	19.9
50–100 kDa	5.4
>100 kDa	5.6

Table 5
Different hydrophilicity fractions distribution of the secondary effluent

Hydrophilicity	Samples (%)
Strong hydrophobic fraction	54.1
Weak hydrophobic fraction	9.6
Charged hydrophilic fraction	25.9
Neutral hydrophilic fraction	10.4

the increases of the filtration time, followed by a long period of a steady value. Experiments were carried out at 0.1 Mpa transmembrane pressure. Reasons that cause the membrane fouling were very complex, owing to the complex water quality of the samples, the different structure, and the properties of membranes. There will be further explanations in the next section.

The various filtration resistances are shown in Fig. 5. As can be seen that the R_t of P2–P4 membrane were lower than that of P1 membrane. It indicates that the addition of cross-linking agent $FeCl_3$ can reduce the membrane resistance effectively. However, the R_t showed an increasing trend with the increasing addition of $FeCl_3$. It could be interpreted that the addition of $FeCl_3$ produced a PVA–Fe^{3+} net work structure, confining the compaction of membrane. And with the increase of Fe^{3+} concentration, the net work structure became denser, resulting in the

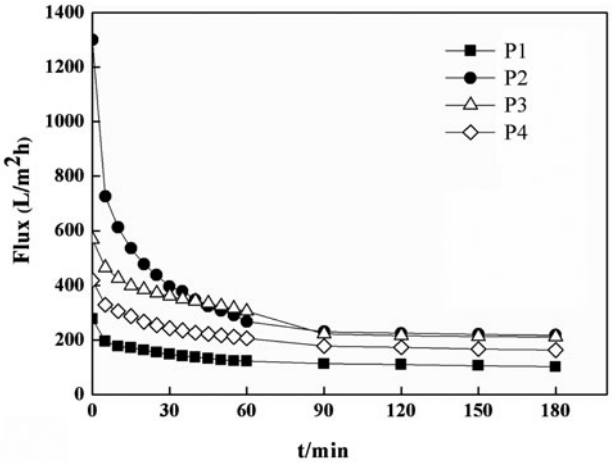

Fig. 4. The decline of permeation flux of different membranes with time increasing.

increase of R_t. The main fouling resistances of the membranes (P2–P4) were attributed to R_c, with the result revealing the formation of cake layer. In addition, the R_f of P2 membrane was the highest and the R_m lowest. The SEM images showed the pore size of P2 membrane was larger than that of other membranes. These indicated that some small molecule pollutants entered into the inner membrane, causing plugging of some pores. This plugging led to flux attenuation and irreversible fouling, bringing a certain degree of influence on flux recovery (see Table 6).

To analyze the contributions of hydrophilicity fractions of the secondary effluent on membrane fouling, the samples of strong hydrophobicity, weak hydrophobicity, charged hydrophilicity, and neutral hydrophilicity were used to filtrate P3 membrane.

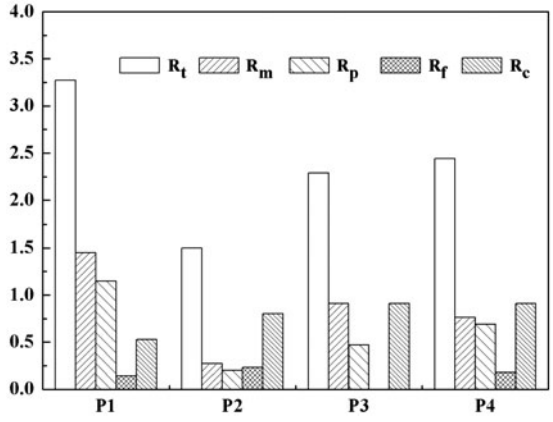

Fig. 5. The filtration resistances of the modified membranes.

Table 6
Flux recovery of backwashing membranes

	Flux recover ratio/%			
Cleaning method	P1	P2	P3	P4
Water washing	91.3	88.5	94	92.1

These samples were labeled as: SH, WH, CH, and NH, respectively. Fig. 6 showed that the permeation flux of membranes declined as the filtration time increased. As can be seen, membrane fouling caused by the charged hydrophilic components of the samples was the most seriously, but its fraction only accounted for 25.9% (see Table 5). While the fraction of strong hydrophobic and weak hydrophobic component accounted for 63.7%, and the membrane pollution degree was also serious. Therefore, the hydrophobic component has a great influence on membrane fouling.

Table 6 shows the flux recovery of backwashing membranes. The flux recovery of all the membranes was high. It may be explained that on the surface of the modified membrane a layer of hydrated layer formed, which can effectively prevent the formation of pollution. Therefore, the results showed the membranes had good antipolluting performance on the secondary effluent.

Table 7 shows that there was no essential difference in the effluent qualities of both membranes. Thus, although the flux of the modified membrane was higher, its performance was not compromised in terms of finished water quality. In summary, the PVA–Fe^{3+} modified membrane was superior to the unmodified

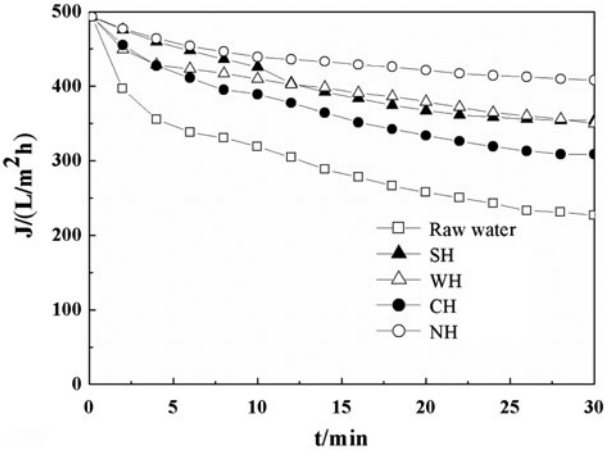

Fig. 6. Filtration behavior of different hydrophobicity components of the water samples.

Table 7
Influent and effluent water qualities for the secondary effluent using the modified membranes

	Influent	Effluent			
		P1	P2	P3	P4
UV_{254}/cm^{-1}	0.16	0.11	0.13	0.11	0.12
$COD/mg\,L^{-1}$	31.2	27.3	28.1	25.6	26.4
$TOC/mg\,L^{-1}$	9.4	8.4	8.5	8.3	7.9
Turbidity/NTU	6	0.03	0.08	0.01	0.02

membrane during filtration due to a higher flux, flux stability, and the long-term stability of the modified membrane will be evaluated in future studies.

4. Conclusions

In summary, the cross-linked PVA/PVDF composite flat sheet membranes were successfully prepared via phase inversion method. With the addition of cross-linking agent $FeCl_3$, the PVA–Fe^{3+} network structure in the membrane was formed, the fouling resistances of the membranes was lower and the water flux was higher. When the weight ratio of PVA to $FeCl_3$ was 1/0.09, the modified membranes had the best UF performance and antifouling property.

Acknowledgments

This research was financially supported by the National Natural Science Foundation of China (Grant No. 51008243, No. 51178378, No. 51278408); Shanxi Province technology and science innovation project (Grant No. 2012KTCL03-06) and the Fund of Shann'xi Educational Committee (2013JK0884).

References

[1] J.G. Jacangelo, R. Rhodes Trussell, M. Watson, Role of membrane technology in drinking water treatment in the United States, Desalination 113 (1997) 119–127.
[2] D. Wang, K. Li, W.K. Teo, Preparation and characterization of polyvinylidene fluoride (PVDF) hollow fiber membranes, J. Membr. Sci. 163 (1999) 211–220.
[3] W.Z. Lang, Z.L. Xu, H. Yang, W. Tong, Preparation and characterization of PVDF–PFSA blend hollow fiber UF membrane, J. Membr. Sci. 288 (2007) 123–131.
[4] K. Dworecki, A. Ślęzak, Evolution of concentration field in a membrane system, J. Biochem. Bioph. Methods 62 (2005) 153–162.
[5] J.R. Du, S. Peldszus, P.M. Huck, X. Feng, Modification of poly(vinylidene fluoride) ultrafiltration membranes with poly(vinyl alcohol) for fouling control in drinking water treatment, Water Res. 43 (2009) 4559–4568.
[6] I. Rubinstein, E. Staude, O. Kedem, Role of the membrane surface in concentration polarization at ion-exchange membrane, Desalination 69 (1988) 101–114.
[7] N. Singh, S.M. Husson, B. Zdyrko, I. Luzinov, Surface modification of microporous PVDF membranes by ATRP, J. Membr. Sci. 262 (2005) 81–90.
[8] M. Masuelli, J. Marchese, N.A. Ochoa, SPC/PVDF membranes for emulsified oily wastewater treatment. J. Membr. Sci. 326 (2009) 688–693.
[9] N. Li, C. Xiao, S. An, X. Hu, Preparation and properties of PVDF/PVA hollow fiber membranes. Desalination 250 (2010) 530–537.
[10] N. Chen, L. Hong, Surface phase morphology and composition of the casting films of PVDF–PVP blend, Polymer 43 (2002) 1429–1436.
[11] A. Linares, A. Nogales, D.R. Rueda, T.A. Ezquerra, Molecular dynamics in PVDF/PVA blends as revealed by dielectric loss spectroscopy, J. Polym. Sci., Part B: Polym. Phys. 45 (2007) 1653–1661.
[12] C.M. Hassan, N.A. Peppas, Structure and applications of poly(vinyl alcohol) hydrogels produced by conventional crosslinking or by freezing/thawing methods, in: Biopolymers PVA hydrogels, anionic polymerisation nanocomposites, Adv. Polym. Sci. 153 (2000) 37–65.
[13] D. Yu. Godovsky, A.V. Varfolomeev, G.D. Efremova, V.M. Cherepanov, G.A. Kapustin, A.V. Volkov, M.A. Moskvina, Magnetic properties of polyvinyl alcohol-based composites containing iron oxide nanoparticles, Adv. Mater. Opt. Electron. 9 (1999) 87–93.
[14] B. Chakrabarty, A.K. Ghoshal, M.K. Purkait, Effect of molecular weight of PEG on membrane morphology and transport properties, J. Membr. Sci. 309 (2008) 209–221.
[15] M. Tomaszewska, Preparation and properties of flat-sheet membranes from poly(vinylidene fluoride) for membrane distillation, Desalination 104 (1996) 1–11.
[16] E.M. Thurman, R.L. Malcolm, Preparative isolation of aquatic humic substances, Environ. Sci. Technol. 15 (1981) 463–466.
[17] S.J. Khan, C. Visvanathan, V. Jegatheesan, Prediction of membrane fouling in MBR systems using empirically estimated specific cake resistance, Bioresour. Technol. 100 (2009) 6133–6136.
[18] Y. Yang, H. Zhang, P. Wang, Q. Zheng, J. Li, The influence of nano-sized TiO_2 fillers on the morphologies and properties of PSF UF membrane, J. Membr. Sci. 288 (2007) 231–238.